Eur. Phys. J. C (2014) 74:2777
DOI 10.1140/epjc/s10052-014-2777-7

THE EUROPEAN PHYSICAL JOURNAL C

Letter

Measuring Dirac CP-violating phase with intermediate energy beta beam facility

P. Bakhti[a], **Y. Farzan**[b]

School of Physics, Institute for Research in Fundamental Sciences (IPM), P.O. Box 19395-5531, Tehran, Iran

Received: 9 July 2013 / Accepted: 5 February 2014 / Published online: 25 February 2014

Abstract Taking the established nonzero value of θ_{13}, we study the possibility of extracting the Dirac CP-violating phase by a beta beam facility with a boost factor $100 < \gamma < 450$. We compare the performance of different setups with different baselines, boost factors, and detector technologies. We find that an antineutrino beam from ^{6}He decay with a baseline of $L = 1300$ km has a very promising CP-discovery potential using a 500 kton water Cherenkov detector. Fortunately this baseline corresponds to the distance between FermiLAB to Sanford underground research facility in South Dakota.

1 Introduction

The developments in neutrino physics in recent 15 years have been overwhelmingly fast. Nonzero neutrino mass has been established and five out of nine neutrino mass parameters have been measured with remarkable precision. In 2012, finally, the relatively small mixing angle, θ_{13} was measured [1–3]. This nonzero value of θ_{13} opens up the possibility of having CP-violating effects in the neutrino oscillations; i.e., $P(\nu_\alpha \to \nu_\beta) \neq P(\bar{\nu}_\alpha \to \bar{\nu}_\beta)$. With this nonzero value of θ_{13}, the quest for measuring the Dirac CP-violating phase, δ_D, has been gathering momentum. A well-studied way to extract δ_D is the precision measurement and comparison of $P(\nu_\mu \to \nu_e)$ and $P(\bar{\nu}_\mu \to \bar{\nu}_e)$ by superbeam and neutrino factory facilities [4]. However, this is not the only way. In fact by studying the energy dependence of just one appearance mode e.g., $P(\nu_\mu \to \nu_e)$, the value of δ_{CP} can be extracted [5]. In [6], a novel method for extracting δ_D (or more precisely $\cos\delta_D$) was suggested that was based on reconstructing the unitary triangle in the lepton sector. The idea of reconstructing the unitary triangle in the lepton sector has been later on studied in [7–13].

[a] e-mail: pouya_bakhti@ipm.ir

[b] e-mail: yasaman@theory.ipm.ac.ir

Recently, beta beam facilities producing ν_e or $\bar{\nu}_e$ beams from the decay of relativistic ions [14–21] have been proposed and studied as an alternative machine to establish CP-violation in the neutrino sector. Most studies were, however, performed before the measurement of θ_{13}, with a focus on the CP-discovery reach for values of θ_{13} much smaller than the measured one [22]. References [23,24] show that using the ν_e beam from ^{18}Ne decay with energies peaked around 1.5–2 GeV, information on δ_D can be extracted without need for an antineutrino beam. In this setup, the boost factor of the decaying ions is $\gamma = 450$. In the present work, we shall consider a similar setup; however, with lower boost factors yielding neutrino energies below the 13-resonance energy in the mantle, which is about 6.5 GeV [25]. For a detailed analysis of the matter effects see [26]. For a neutrino beam with a given energy in the range 400 MeV $< E_\nu <$ 1.5 GeV, the oscillation probability can be approximately written as

$$P_{e\mu} \simeq |c_{12}^m c_{23}(e^{i\lambda_2} - e^{i\lambda_1}) + s_{13}^m s_{23} e^{-i\delta_D}(e^{i\lambda_3} - e^{i\lambda_2})|^2 \tag{1}$$

where $c_{12}^m \ll 1$ is the cosine of the 12-mixing angle in matter and λ_i are the phases resulting from the propagation; i.e., for a constant density $\lambda_i = (m_i^2)_{\rm eff} L/(2E)$. For the antineutrino mode, a similar equation holds with $s_{12}^m \ll 1$ and

$$P_{\bar{e}\bar{\mu}} \simeq |s_{12}^m c_{23}(e^{i\lambda_2} - e^{i\lambda_1}) + s_{13}^m s_{23} e^{i\delta_D}(e^{i\lambda_3} - e^{i\lambda_1})|^2. \tag{2}$$

Notice that in the above formulas, the deviations of the values of θ_{23} and δ_D in matter from those in vacuum are neglected. These deviations are of order of $\Delta m_{12}^2/\Delta m_{13}^2$ [26]. As long as $|\lambda_2 - \lambda_1| \sim 1$, the two terms in Eq. (1) as well as those in Eq. (2) are of the same order so the interference terms which are sensitive to δ_D are of order of the oscillation probabilities themselves. This means that the variation in the oscillation probabilities due to the change of δ_D within $(0\,\pi)$ is of order of the oscillation probabilities, themselves. As a result for these energies and $|\lambda_2 - \lambda_1| \sim 1$, even a moderate precision

in the measurement of the probabilities will be enough to extract the value of δ_D.

The flux at the detector scales as γ^2 and the scattering cross section of neutrinos increases by increasing the energy (i.e., increasing γ). As a result, for a given baseline, the statistics increases with γ. Based on this observation, most attention in recent years has been given to $\gamma > 300$. However, one should bear in mind that for $\gamma < 300$, there is the advantage of using very large water Cherenkov (WC) detectors. In this energy range, the neutrino interaction will be dominantly quasi-elastic and its scattering cross section is known with high precision.

In the literature, the CP-discovery potential of a beta beam setup from CERN to Frejus with $\gamma < 150$ and $L = 130$ km has been investigated [27]. Moreover, varying the values of γ and baselines, it has been shown that for $150 < \gamma < 300$ with 500 kton WC detector [28–30] or iron calorimeter [31], there is a very good chance of CP-discovery. Reference [22] explores the θ_{13}–δ_D-discovery reach with a 300 kton WC and 50 kton LAr detector at Deep Underground Science and Engineering Laboratory (DUSEL), taking maximum boosts possible at Tevatron. Now that the value of θ_{13} is measured and found to be sizeable, reconsidering $\gamma < 300$ setup is imperative. In vacuum, the dependence of the oscillation probability on L and γ would be through L/γ. However, for setups under consideration, because of the matter effects, the dependence on L and γ is more sophisticated so the dependence on E and L has to be investigated separately. In particular, while Ref. [28] focuses on $L/\gamma = 2.6$ km, we have found that for $L/\gamma > 2.6$ km, there is a very good discovery potential. The present paper is devoted to such a study.

In Sect. 2, we describe the inputs and how we carry out the analysis. We outline the characteristics of the beam and the detector as well as the sources of the background and the systematic errors. In Sect. 3, we present our results and analyze them. In Sect. 4, we summarize our conclusions and propose an optimal setup for the δ_D measurement.

2 The inputs for our analysis

Using the GloBES software [32,33], we investigate the CP-discovery potential of a beta beam setup with various baselines and beam boost factors, γ. For the central values of the neutrino parameters, we have taken the latest values in Ref. [34]. The hierarchy can be determined by other experiments such as PINGU [35–41] or combining PINGU and DAYA Bay II results [42], so we assume that this hierarchy is known by the time that such a beta beam setup is ready. We study both normal and inverted hierarchies. T2K and Nova can also solve the octant degeneracy and determine whether $\theta_{23} < 45°$ or $\theta_{23} > 45°$ [43]. The data already excludes the $\theta_{23} > 45°$ solution at 1σ CL. For the uncertainty of the mixing parameters, we take the values that will be achievable by forthcoming experiments. Namely, we take the following uncertainties: 0.4 % for θ_{12} [44], 1.8 % for θ_{13} [45], 2 % for θ_{23} [46], 0.2 % for Δm^2_{12} [44] and 0.7 % for Δm^2_{13} [35–40]. As predefined by GLoBES, we use the matter profiles in [47,48]. We consider 5 % error for matter density. The uncertainties are treated by the so-called pull-method [32,33]. While the effects of uncertainty in matter density is more important for larger baselines, the uncertainties of neutrino parameters affect the results from smaller baselines more.

As the source of neutrino (antineutrino) beam, we take decays of ^{18}Ne (^{6}He):

$$^{18}\mathrm{Ne} \rightarrow {}^{18}\mathrm{F} + \mathrm{e}^+ + \nu_\mathrm{e}$$

and

$$^{6}\mathrm{He} \rightarrow {}^{6}\mathrm{Li} + \mathrm{e}^- + \bar{\nu}_\mathrm{e}.$$

The endpoint energies of these two decays are very close to each other: $E_0 = 3.4$ MeV for ^{18}Ne and $E_0 = 3.5$ MeV for ^{6}He. As a result for equal γ, the energy spectrum of ν_e and $\bar{\nu}_\mathrm{e}$ from their decays will be approximately similar. The pair of ^{8}Li and ^{8}B isotopes have also been discussed in the literature as a potential source of the ν_e and $\bar{\nu}_\mathrm{e}$ beams. In these cases, the endpoints are higher so as to have neutrino beams with energies $E_\nu < 1.5$ GeV, the values of γ should be lower than in the case of ^{18}Ne/^{6}He. On the other hand, the flux at the detector drops as γ^{-2} so with the ^{8}Li and ^{8}B isotopes, the number of decays should be larger to compensate for the γ^{-2} suppression. We will not consider the ^{8}Li/^{8}B isotopes in this paper and will focus on the ^{18}Ne/^{6}He pair. For the neutrino (antineutrino) mode, we take 2.2×10^{18} (5.8×10^{18}) decays of ^{18}Ne (^{6}He) per year, which seems to be realistic [49]. The Tevatron accelerator can accelerate ^{18}Ne and ^{6}He up to boost factors 586 and 351, respectively.

While the disappearance probabilities (i.e., $P(\nu_\mathrm{e} \rightarrow \nu_\mathrm{e})$ or $P(\bar{\nu}_\mathrm{e} \rightarrow \bar{\nu}_\mathrm{e})$) are not sensitive to δ_D, the appearance probabilities (i.e., $P(\nu_\mathrm{e} \rightarrow \nu_\mu)$ or $P(\bar{\nu}_\mathrm{e} \rightarrow \bar{\nu}_\mu)$) contain information on δ_D. In our analysis, we, however, employ both appearance and disappearance modes. In principle, the disappearance mode can help to reduce the effect of uncertainty in other parameters but we have found that the effect of turning off the disappearance mode on the δ_D measurement is less than 1 %. To derive the value of δ_D, the detector has to distinguish ν_μ from ν_e. We focus on a 500 kton water Cherenkov (WC) detector and compare its performance with a 50 kton totaly active scintillator detector (TASD).

In the energies of our interest with $\gamma < 300$, the main interaction mode is Charged Current (CC) quasi-elastic mode with a non-negligible contribution from inelastic charged current interaction which produce one or more pions along with the charged lepton. In principle, the quasi-elastic CC events can be distinguished from the inelastic CC ones by counting the number of Cherenkov rings. However, to dis-

tinguish the two interactions with a WC detector will be challenging. We take the signal to be composed of both quasi-elastic and inelastic charged current events and conservatively assume that the WC detector cannot distinguish between the two.

In the case of QE interaction by measuring the energy and the direction of the final charged lepton, the energy of the initial neutrino can be reconstructed up to an uncertainty of 0.085 GeV, caused by the Fermi motion of the nucleons inside the nucleus. However, in the inelastic interaction, a fraction of the initial energy is carried by pions, so the energy of the initial neutrino cannot be reconstructed by measuring the energy and the direction of the final lepton alone. A WC detector cannot measure the energy deposited in hadronic showers, so with this technique the reconstruction of the energy spectrum will be possible only for the QE interactions. Following the technique in [28,50] we take an unknown normalization for QE events and use its spectrum as a basis for energy reconstruction. Of course, with this method energy reconstruction cannot be carried out on an event by event basis and information on the spectrum will only be statistical. TASD can measure the energy deposited in hadronic showers, too. As a result, energy reconstruction by TASD can be possible on an event by event basis.

As shown in [51], the background from atmospheric neutrinos can be neglected and the main source of background for both TASD and WC detectors are neutral current interactions of the beam neutrinos. In our analysis, for the cross sections of the quasi-elastic, inelastic and neutral current interactions we employ the results of [52,53]. Recently the MiniBooNE collaboration has measured the antineutrino cross section in the energy range of our interest [54] with remarkable precision. In the near future, the measurement of the cross section will become even more precise. Unless otherwise stated, we assume 4 years of data taking.

For the treatment of the efficiencies and backgrounds we implement the same methods as used in [28,50]. While for the purpose of this paper the methods used in [28,50] are adequate, we would like to note that a more complete discussion of reconstruction of events in the large WC detectors can be found in [51]. To be more specific, similarly to [28] we assume the following characteristics for the WC detector performance. We take a signal efficiency of 55 % for neutrinos and of 75 % for antineutrinos. We take the uncertainty in the normalization of the total signal to be 2.5 % but as we mentioned above, we take a free normalization for QE events. We assume a background rejection of 0.3 % for neutrinos and 0.25 % for antineutrinos. The normalization uncertainty of the background is taken to be 5 %. For both background and signal, the calibration error is 0.0001. For the energy reconstruction of the background, we use the migration matrices tabulated for the GLoBES package [55,56]. We consider the energy range between 0.2 and 3 GeV and divide it into 28 bins. The energy resolution for QE CC interactions is assumed to be of the form $0.085 + 0.05\sqrt{E/\text{GeV}}$ GeV for both muon and electron neutrino detection. The first term originates from the Fermi motion of the nucleons inside nuclei and the second term reflects the error in measuring the energy of the final charged lepton [22].

As in Ref. [28], we assume the following features for TASD: A signal efficiency of 80 % for ν_μ and $\bar{\nu}_\mu$ and of 20 % for ν_e and $\bar{\nu}_e$; background rejection of 0.1 %; a signal normalization uncertainty of 2.5 %; normalization uncertainty of 5 %; a calibration error of 0.0001. The energy resolution is given by $0.03\sqrt{E/\text{GeV}}$ GeV for muon (anti)neutrinos and $0.06\sqrt{E/\text{GeV}}$ GeV for electron (anti)neutrinos. The energy range is taken to be 0.5–3.5 GeV and is divided into 20 bins. We have studied the dependence of our results on the number of bins. It seems that the results do not change by increasing the number of bins to 30.

3 Results and the interpretation

In Figs. 1 and 3, the vertical axis shows the precision with which $\delta_D = 90^\circ$ can be determined at 1σ % CL. We take $\delta_D = 90^\circ$ and define $\Delta\delta_D$ to be the range for which $\Delta\chi^2 < 1$. More precisely, $\Delta\delta_D$ is defined as the difference between maximum and minimum values of δ_D around $\delta_D = 90^\circ$ for which $\Delta\chi^2 = 1$. From Fig. 1, we observe that the low energy setup with $\gamma = 300$ and WC detector can outperform the setup with $\gamma = 450$ and TASD detector for both normal and inverted hierarchies. The oscillatory behavior of the curves is driven by the 13-splitting and has a frequency given by $\sim \Delta m^2_{31}/(2E)$. Such a behavior can be understood by the following consideration on Eqs. (1) and (2): While $\lambda_2 - \lambda_1$ is driven by $(\Delta m^2_{21})_{\text{eff}}$ and slowly varies with L, $\lambda_3 - \lambda_2$ is driven by $(\Delta m^2_{32})_{\text{eff}}$ and varies rapidly. For the values of L with $\lambda_3 - \lambda_2 = 2n\pi$, the sensitivity is lost. This consideration explains the oscillatory behavior of Fig. 1. Notice, however, that this consideration holds for a given E_ν. If the energy spectrum is wide, the effect will smear out. In other words, if the number of energy bins from which information on δ_D can be deduced (i.e., the bins for which the number of events without oscillation is sizeable and the quasi-elastic interactions dominate) is relatively large, missing information in few of these bins for which $(\lambda_3 - \lambda_2) \to 0$ will not affect much the precision in the determination of δ_D. In the opposite case, when at all such bins $(\lambda_3 - \lambda_2) \to 0$, the precision in δ_D will be dramatically deteriorated. Increasing the boost factor increases both the peak energy and the energy width. Thus, we expect for higher γ that the oscillatory behavior is to be smeared out. Figure 1 confirms this expectation. In the case of antineutrinos, the information on δ_D can be deduced from a larger range of the spectrum mainly because of the shape of the spectrum at the source and the fact that for antineutrinos,

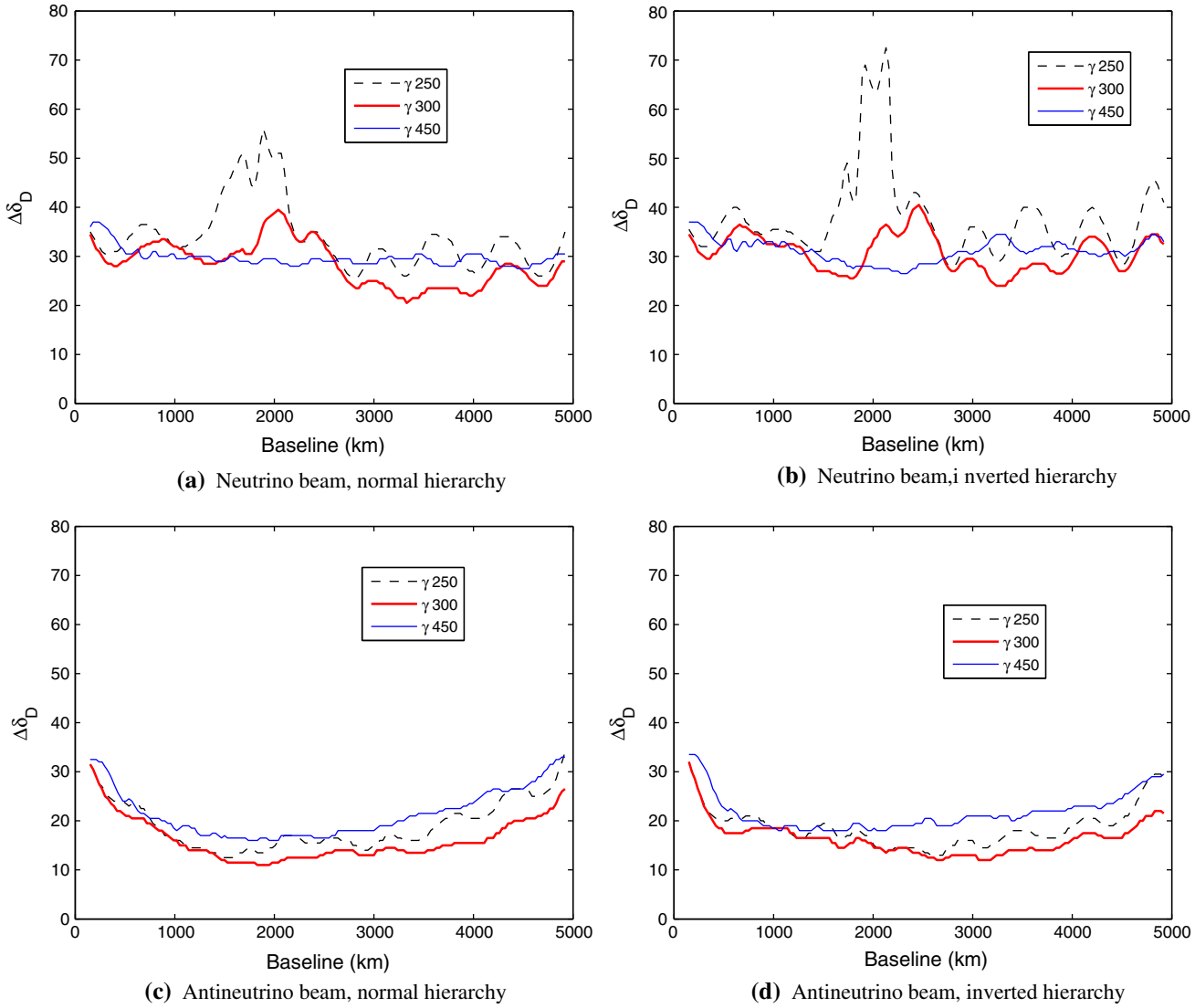

(a) Neutrino beam, normal hierarchy

(b) Neutrino beam,i nverted hierarchy

(c) Antineutrino beam, normal hierarchy

(d) Antineutrino beam, inverted hierarchy

Fig. 1 Uncertainty within which $\delta_D = 90^\circ$ can be measured at 1σ CL after 4 years of data taking versus baseline for different values of the boost factor. For $\gamma = 450$, a 50 kton TASD detector and for lower γ, a 500 kton WC detector are assumed. In the *upper* (*lower*) panels, a neutrino (antineutrino) beam with 2.2×10^{18} (5.8×10^{18}) decays per year is assumed. In the *left* (*right*) panels, the hierarchy is taken to be normal (inverted). We have taken the true values for the left panels as $\Delta m^2_{31} = 2.421 \times 10^{-3}$ eV^2 (normal hierarchy) and $\theta_{23} = 41.4^\circ$ (first octant). For the right panels we have taken $\Delta m^2_{31} = -2.35 \times 10^{-3}$ eV^2 (inverted hierarchy) and the same mixing angles

the QE interactions dominate over the inelastic interaction for a wider energy range compared to the case of neutrino [52,53]. As a result, the modulation driven by Δm^2_{31} is less severe for antineutrinos. As seen in the lower panels of Fig. 1, the antineutrino beam with $\gamma = 300$ and a WC detector can achieve an impressive precision of better than 20° for baselines over 500 km.

Figure 2 shows the fraction of the parameter δ_D for which CP-violation can be established. From these figures, we also observe that setups with $\gamma < 300$ and a 500 kton WC detector can outperform the setup with a 50 kton TASD detector and $\gamma = 450$ for $L < 2500$ km.

Figures 3 and 4 compare the CP-discovery potential of a ν run with an $\bar{\nu}$ run and a mixed balanced run. For the antineutrino run the decay rate is taken to be about 2.6 times that of neutrinos to compensate for the low cross sections of antineutrinos. For 200 km $< L <$ 5000 km, the antineutrino run seems to outperform both the neutrino run and the mixed run in the precision measurement of $\delta_D = 90^\circ$. This result is at odds with the results of [28]. However, we should remember that Ref. [28] focuses on a specific value of L/γ. In this energy and baseline range, the sensitivity of the average $P(\bar{\nu}_e \to \bar{\nu}_\mu)$ to δ is higher than that of the average $P(\nu_e \to \nu_\mu)$.

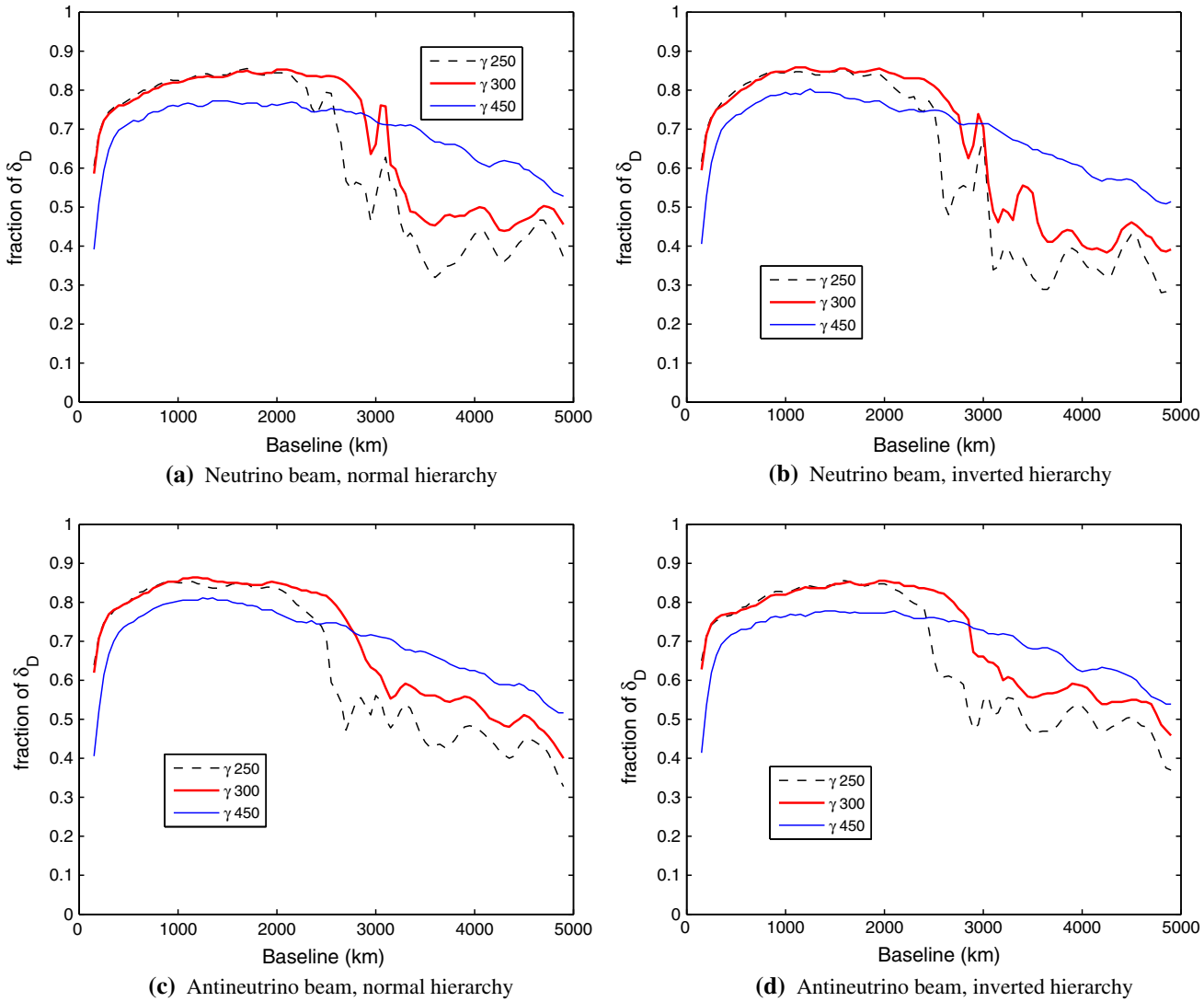

(a) Neutrino beam, normal hierarchy

(b) Neutrino beam, inverted hierarchy

(c) Antineutrino beam, normal hierarchy

(d) Antineutrino beam, inverted hierarchy

Fig. 2 The fraction of the δ_D parameter for which CP can be established at higher than 95 % CL after 4 years of data taking versus baseline. The rest of description is as in Fig. 1

For $L = 1300$ km, (corresponding to the baseline of the LBNE setup from the FermiLAB to Sanford underground research facility in South Dakota [57]), we also observe that $\gamma = 300$ with WC detector is promising and can outperform the $\gamma = 450$ setup with TASD detector. Figure 5 shows $\Delta\delta_D$ versus γ for $L = 1300$ km and $L = 2300$ km. The latter corresponds to the baseline for the LBNO setup from CERN to Finland [58]. The plots show that the setup with $\gamma = 200{-}300$ and $L = 1300$ km can measure $\delta_D = 90°$ with a remarkable precision and also have an outstanding coverage of the δ_D range. At this baseline, increasing γ from 200 to 300 does not much improve the sensitivity to δ_D.

For relatively short baselines $L \sim 100$ km, $\sin(\lambda_2 - \lambda_1)/2 \ll 1$, so the contributions of the first terms in Eqs. (1) and (2) are subdominant relative to the second terms. As a result, the interference between the first and second terms which is the only contribution sensitive to δ_D will be suppressed; i.e., when δ_D varies between 0 and π the variation of $P_{e\mu}$ and $P_{\bar{e}\bar{\mu}}$ will be of order of $\sin(\lambda_2 - \lambda_1)/2 \sim 0.05L/(130\ \text{km})$. On the other hand, for $L > 1000$ km, $\sin(\lambda_2 - \lambda_1)/2 \sim 1$ and the two terms in Eqs. (1) and (2) are of the same order, making the variation of the oscillation probabilities due to the variation of δ_D of order of the oscillation probabilities themselves. As a result, deriving δ_D from a 130 km setup such as CERN to Frejus requires a different strategy than that of a very long baseline setup with $L > 1000$ km. This is demonstrated in Figs. 5 and 6. From Fig. 5 we observe that the pure $\bar{\nu}_e$ run in the case of the setup with $L = 1300$ km has a better prospect but as seen in Fig. 6, in the case of the $L = 130$ km baseline a mixed run of neutrino and antineutrino can perform better than pure ν_e or $\bar{\nu}_e$ runs. For $\sin(\lambda_2 - \lambda_1)/2 \ll 1$, the uncertainties in

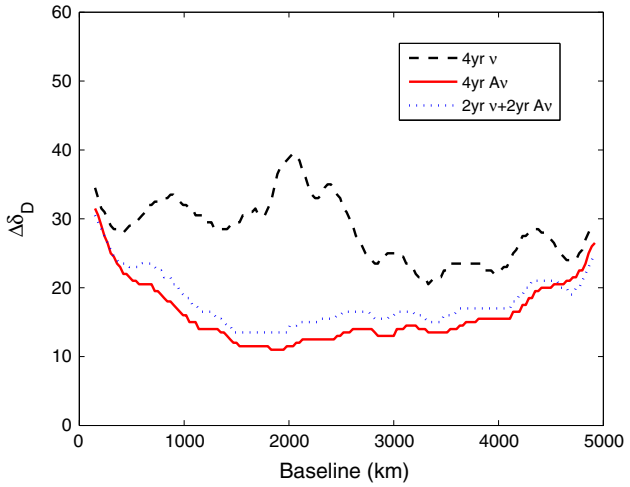

Fig. 3 Uncertainty within which $\delta_D = 90°$ can be measured versus baseline at 1σ CL. The neutrino parameters are as in Fig. 1. The hierarchy is taken to be normal. For the neutrino and antineutrino beams, 2.2×10^{18} and 5.8×10^{18} decays per year are assumed, respectively. The curves shown with the *dashed* and *solid lines*, respectively, show the results of 4 years run in neutrino mode from the ^{18}Ne decay and 4 years run in antineutrino mode from the ^{6}He decay. The curve shown by *dotted line* displays the results of 2 years of neutrino run combined with 2 years of antineutrino run. The boost factors of the beams are taken to be 300

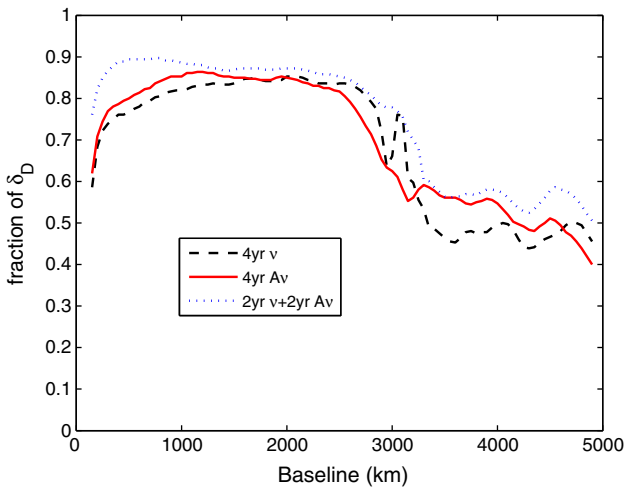

Fig. 4 The fraction of the δ_D parameter for which CP can be established at higher than 95 % CL versus baseline. The rest of the description is as that of Fig. 3

neutrino parameters (especially the uncertainties of θ_{13} and θ_{23}) induce a significant uncertainty in the derivation of δ_D. If we turn off the error in these parameters, the performance of the CERN to Frejus setup will be competitive with that of the LBNE setup, but considering the realistic uncertainty in these parameters as outlined in the previous section, the sensitivity of the LBNE setup to δ_D is much better than the $L = 130$ km setup. This can be confirmed by comparing Figs. 5 and 6.

For the 130 km setup, the oscillation probabilities can be approximately written as $P_{\bar{e}\bar{\mu}} \simeq |is^m_{12}c_{23}\sin(\lambda_2 - \lambda_1) + s^m_{13}s_{23}e^{i\delta_D}(e^{i\lambda_3} - 1)|^2$ and $P_{e\mu} \simeq |ic^m_{12}c_{23}\sin(\lambda_2 - \lambda_1) + s^m_{13}s_{23}e^{-i\delta_D}(e^{i\lambda_3} - 1)|^2$. Since we are far from the 31-resonance, s^m_{13} is not very different from s_{13} and is approximately the same for normal and inverted hierarchies. As a result, replacing $\delta_D \to \pi - \delta_D$ and $\Delta m^2_{13} \to -\Delta m^2_{13}$ (i.e., $\lambda_3 \to -\lambda_3$), the oscillation probability does not change. That is why in Fig. 6 the $\Delta\delta_D$ plots for normal and inverted hierarchies are practically the same. If we take a value other than 90° as the true value of δ_D, we will not have such a symmetry. However, as seen in Figs. 5 and 6, the general behavior for normal and inverted hierarchies are similar. With the present SPS setup, CERN cannot enhance γ over 150 for the ^{6}He ions [29]. On the other hand, from Fig. 6, we observe that with $L = 130$ km, there is no point in seeking higher values of γ. In fact, at $\gamma = 150$, the fraction of CP-violating δ_D parameter for which CP-violation can be established is slightly higher than that for $\gamma > 250$.

From comparing Figs. 5 and 6, we observe that the best performance can be achieved by an $L = 1300$ km setup and antineutrino run. For example, while with the CERN to Frejus setup, $\delta_D = 90°$ can be measured with only an uncertainty of $\Delta\delta_D = 35°$, with a 1,300 km setup, the uncertainty can be lowered down to $\Delta\delta_D = 15°$. Notice that for these setups, the same detector (500 kton WC) is assumed. Although with longer baselines the flux decreases, instead $\lambda_2 - \lambda_1$ in Eq. (2) becomes larger, so a moderate precision in the $P_{\bar{e}\bar{\mu}}$ measurement will suffice to extract δ_D. For measuring $\delta_D = 90°$, the $L = 2300$ km setup with the $\bar{\nu}_e$ run seems to be competitive with the $L = 1300$ km setup; however, the fraction of δ_D to be established by the $L = 1300$ km setup is considerably higher. Among the setups that we have considered the $L = 1300$ km setup with a 500 kton WC and the $\bar{\nu}$ run seems to be the most promising one. In Fig. 5, we observe that for $200 < \gamma < 300$, the curves corresponding to the $\bar{\nu}_e$ run are almost flat.

As expected for $L > 1000$ km, the results are highly sensitive to the central values of Δm^2_{31}. The oscillatory behavior in Fig. 1 that we discussed before implies such a sensitivity. In fact, the setup that we are proposing can simultaneously extract δ_D and Δm^2_{31}. Figure 7 shows 68 and 95 % CL contours for $\gamma = 300$ and $L = 1300$ km (LBNE). In drawing these plots, the hierarchy is assumed to be known; however, the measured value of Δm^2_{31} is not used. The precision in Δm^2_{31} can drastically be improved by forthcoming experiments. In [41], it is shown that combining the T2K and PINGU results, 0.7 % precision in Δm^2_{31} is achievable. In Fig. 7 the vertical lines show the 0.7 % uncertainty in Δm^2_{31} around the 'true' value of Δm^2_{31}. As seen from the figure, for the case of the antineutrino beam the uncertainty in Δm^2_{31} will not significantly increase the uncertainty in the δ_D determination.

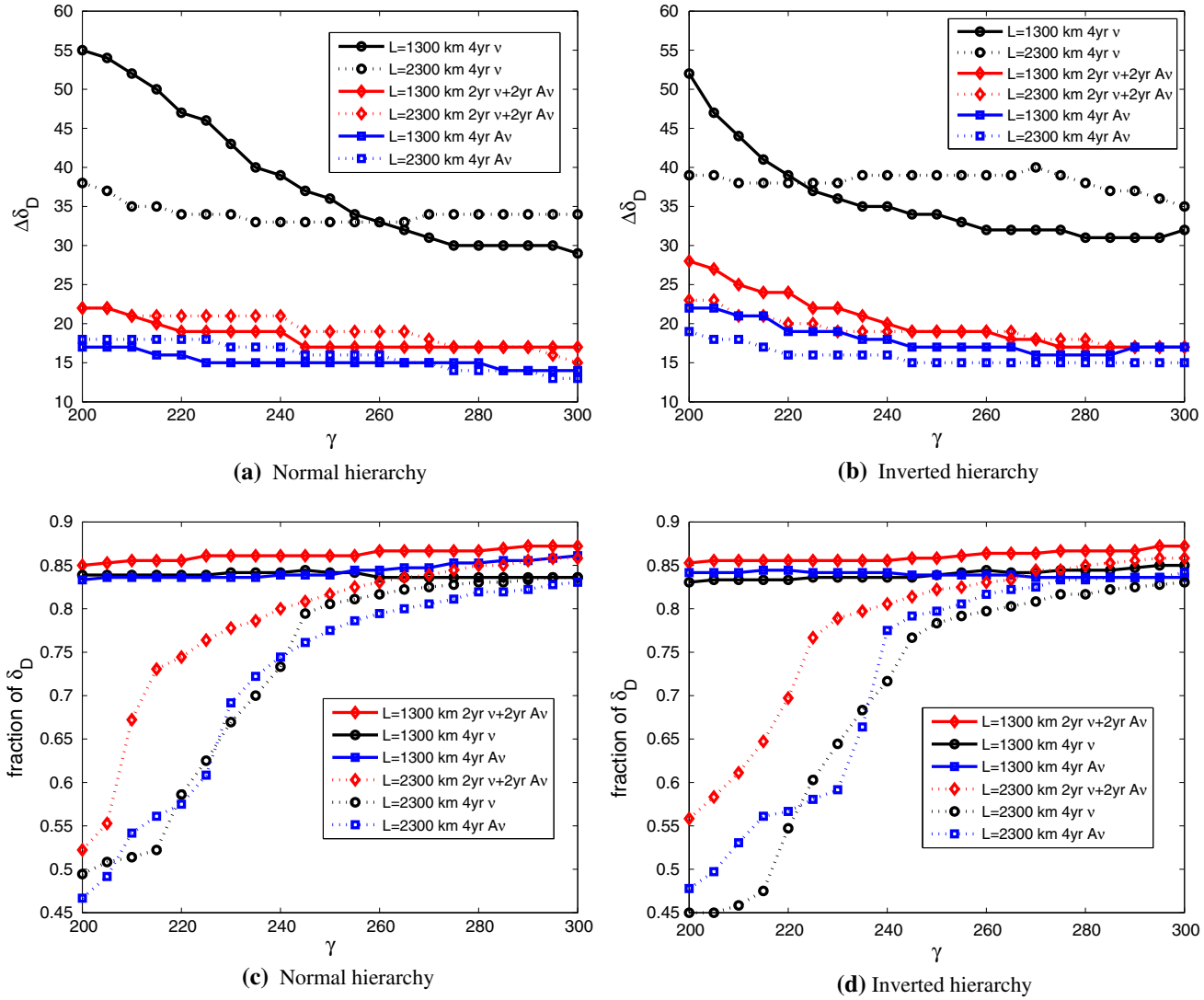

(a) Normal hierarchy

(b) Inverted hierarchy

(c) Normal hierarchy

(d) Inverted hierarchy

Fig. 5 The CP-discovery potential by the setups with baselines equal to 2,300 and 1,300 km after 4 years of data taking versus the boost factors of the neutrino and antineutrino beams. In the *left* (*right*) panels, the hierarchy is taken to be normal (inverted). *Upper panels* the uncertainty within which $\delta_D = 90°$ can be measured at 1σ CL versus the boost factors of ν_e and $\bar{\nu}_e$ beams from the ^{18}Ne and ^{6}He decay. *Lower panels* the fraction of the δ_D parameter for which CP can be established at higher than 95 % CL

4 Conclusions

Measuring the CP-violating phase by a beta beam facility has been extensively studied in the literature. Most of the recent studies have focused on relatively high energy beams with $\gamma > 300$. The reason is that for a given baseline, the number of detected neutrinos increases approximately as γ^3. However, for lower energy beta beam, a large volume WC detectors [30] can be employed that can compensate for the decrease of flux and cross section. Moreover, with the relatively large value of θ_{13} chosen by Nature, having enough statistics will not be the most serious challenge for measuring the CP-violating phase. Considering these facts, we have explored the CP-discovery reach of an intermediate energy beta beam for various baselines and different neutrino vs. antineutrino combinations using the GLoBES software [32,33]. We have discussed the precision with which δ_D can be measured, assuming that by the time that the required facilities are ready the hierarchy is also determined. Our results do not depend much on which mass ordering is chosen.

We have found that a setup with only an antineutrino run with $200 < \gamma < 300$ and a baseline of $L = 1,300$ km has an excellent discovery potential. Four years run of such a setup with 5.8×10^{18} ^{6}He decays per year can establish CP-violation at 95 % CL for more than 85 % of the δ_D parameter range. If $\delta_D = 90°$, this setup can determine it with impressive precision $\delta_D = 90° \pm 8°$ for an inverted hierarchy and

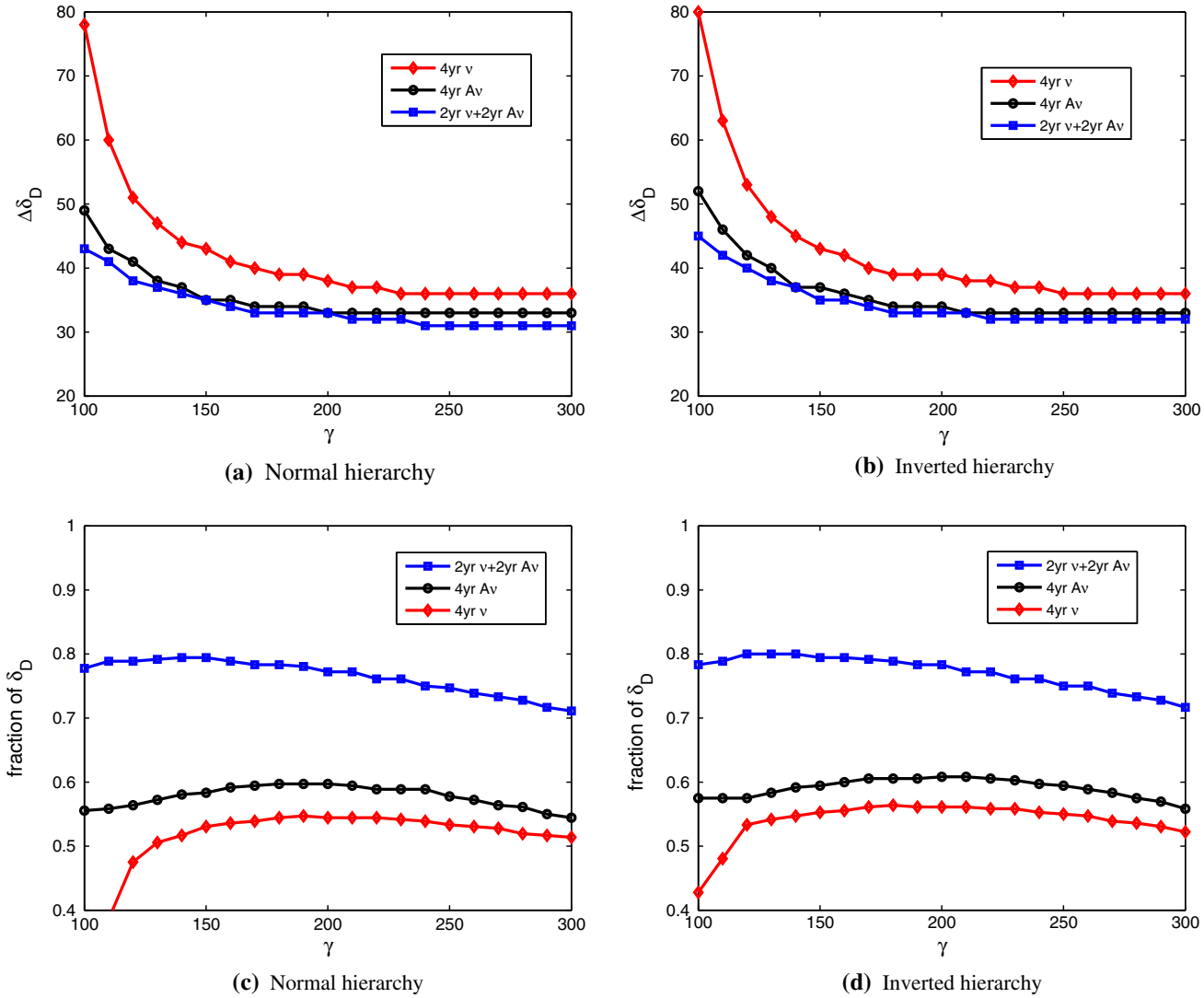

(a) Normal hierarchy

(b) Inverted hierarchy

(c) Normal hierarchy

(d) Inverted hierarchy

Fig. 6 The CP-discovery potential of a 130 km experiment (distance between CERN to Frejus) after 4 years of data taking versus the boost factors of neutrino and antineutrino beams. In the *left* (*right*) panels, the hierarchy is taken to be normal (inverted). *Upper panels* the uncertainty within which $\delta_D = 90°$ can be measured at 1σ CL versus the boost factors of the ν_e and $\bar{\nu}_e$ beams from the ^{18}Ne and ^{6}He decay. *Lower panels* the fraction of the δ_D parameter for which CP can be established at higher than 95 % CL

$\delta_D = 90° \pm 7°$ for a normal hierarchy at 1σ CL. Such a baseline corresponds to the distance between FermiLAB to Sanford underground research facility in South Dakota. A baseline of $L = 1300$ km seems to be close to the optimal distance to measure the Dirac CP-violating phase. We have found that for this baseline a setup with intermediate values of γ in the range $200 < \gamma < 300$ with a 500 kton WC detector can outperform that with $\gamma = 450$ and 50 kton TASD.

For very long baselines with $L > 1000$ km, a pure antineutrino source from ^{6}He enjoys a better performance than a mixed neutrino antineutrino run. On the other hand for shorter baselines, a balanced neutrino–antineutrino mode gives better results. We have specifically discussed the CERN to Frejus setup with $L = 130$ km baseline. We have found that with 2 years of neutrino mode from 2.2×10^{18} decays of ^{18}Ne per year combined with 2 years of antineutrino mode from 5.8×10^{18} decays of ^{6}He per year both with $\gamma = 150$ (the largest boost that can be obtained for ^{6}He with the present SPS accelerator at CERN [29]), the CP-violation can be established for about 80 % of the δ_D parameter range. With such a setup and runtime, if the true value of δ_D is equal to 90°, it can be measured as $\delta_D = 90° \pm 18°$ at 1σ CL. By increasing γ to higher values, the precision in the δ_D measurements slightly improves, however, still with a similar detector and antineutrino run, the performance of $L = 1,300$ km can be better.

Our conclusion is that a beta beam facility with $200 < \gamma < 300$, a baseline of $L \simeq 1300$ km, and 500 kton WC run-

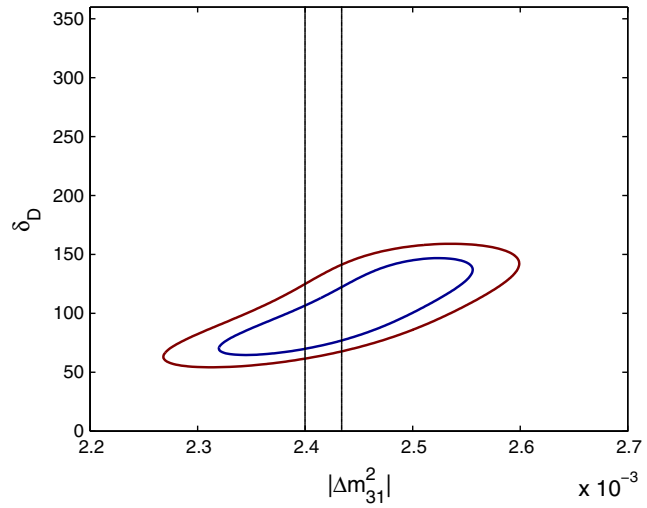

(a) Neutrino beam, normal hierarchy

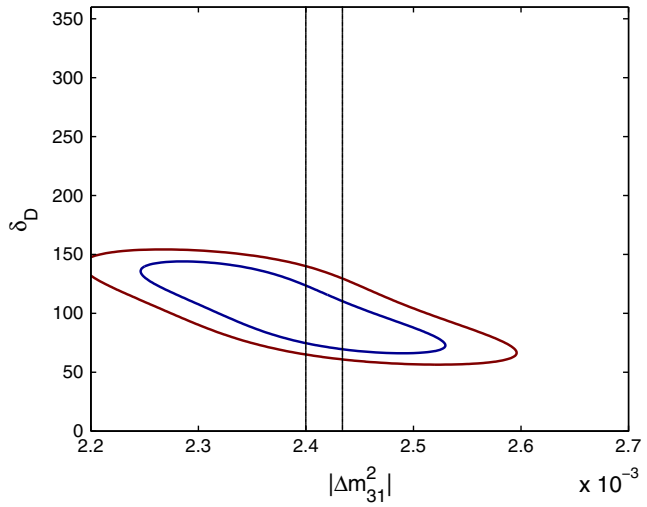

(b) Neutrino beam, inverted hierarchy

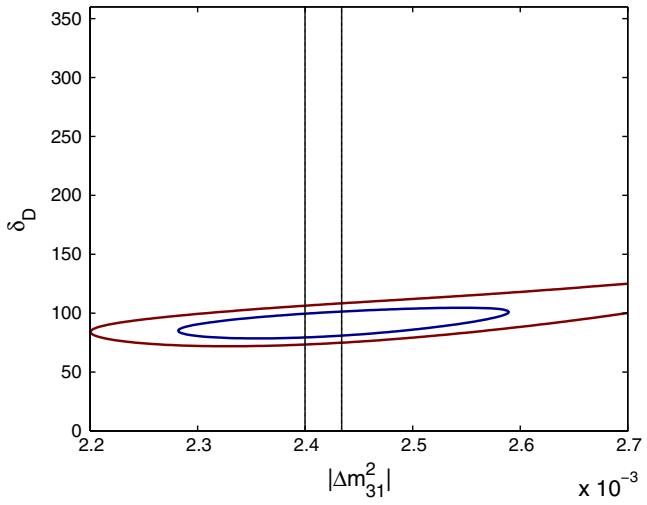

(c) Antineutrino beam, normal hierarchy

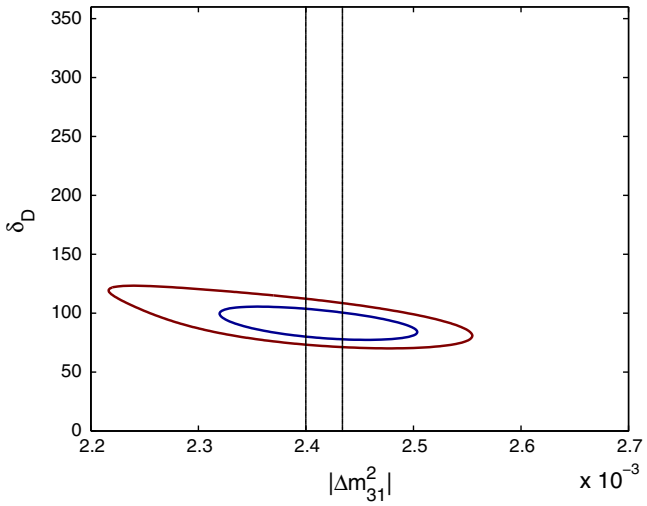

(d) Antineutrino beam, inverted hierarchy

Fig. 7 Determination of δ_D and Δm^2_{31} with $\gamma = 300$ and $L = 1300$ km after 4 years of data taking. The contours show 68 % CL and 95 % CL. In the *upper* (*lower*) panels, a neutrino (antineutrino) beam with 2.2×10^{18} (5.8×10^{18}) decays per year is assumed. In the *left* (*right*) panels, the hierarchy is taken to be normal (inverted). The true value of δ_D is taken to be 90°. For a normal (inverted) hierarchy, we take $\Delta m^2_{31} = 2.421 \times 10^{-3}\text{eV}^2$ ($\Delta m^2_{31} = -2.35 \times 10^{-3}\text{eV}^2$). The *vertical lines* show a 0.7 % uncertainty in Δm^2_{31} (e.g., for the normal hierarchy $\Delta m^2_{31} = 2.421 \times 10^{-3}\,\text{eV}^2 \times (1 \pm 0.7\ \%)\ \text{eV}^2$)

ning in the antineutrino mode from ^{6}He decay is an optimal option for establishing CP-violation in the lepton sector and the measurement of δ_D. The location of source and detector might be, respectively, FermiLAB and Sanford underground laboratory in South Dakota.

Acknowledgments The authors would like to thank A. Yu. Smirnov for encouragement and very useful comments. They also thank F. Terranova and W. Winter for fruitful comments. P. B. acknowledges H. Mosadeq for technical help in running the computer codes. They also acknowledges partial support from the European Union FP7 ITN INVISIBLES (Marie Curie Actions, PITN-GA-2011-289442). Y.F. thanks the staff of Izmir technical institute (IZTECH) where a part of this work was carried out for generous support and hospitality. The authors also thank the anonymous referee for useful remarks.

References

1. F.P. An et al. [DAYA-BAY Collaboration], Phys. Rev. Lett. **108**, 171803 (2012). arXiv:1203.1669 [hep-ex]
2. J.K. Ahn et al. [RENO Collaboration], Phys. Rev. Lett. **108**, 191802 (2012). arXiv:1204.0626 [hep-ex]
3. Y. Abe et al. [DOUBLE-CHOOZ Collaboration], Phys. Rev. Lett. **108**, 131801 (2012). arXiv:1112.6353 [hep-ex]

4. A.Bandyopadhyay et al. [ISS Physics Working Group Collaboration], Rept. Prog. Phys. **72**, 106201 (2009). arXiv:0710.4947 [hep-ph]
5. M.V. Diwan, D. Beavis, M.-C. Chen, J. Gallardo, S. Kahn, H. Kirk, W. Marciano, W. Morse et al., Phys. Rev. D **68**, 012002 (2003). hep-ph/0303081
6. Y. Farzan, A.Y. Smirnov, Phys. Rev. D **65**, 113001 (2002). hep-ph/0201105
7. H. Zhang, Z.-z. Xing, Eur. Phys. J. C **41**, 143 (2005). hep-ph/0411183
8. A. Bandyopadhyay et al. [ISS Physics Working Group Collaboration], Rept. Prog. Phys. **72**, 106201 (2009). arXiv:0710.4947 [hep-ph]
9. G. Ahuja, M. Gupta, Phys. Rev. D **77**, 057301 (2008). hep-ph/0702129 [HEP-PH]
10. Z.-z. Xing, H. Zhang, Phys. Lett. B **618**, 131 (2005). hep-ph/0503118
11. S. Antusch, S.F. King, C. Luhn, M. Spinrath, Nucl. Phys. B **850**, 477 (2011). arXiv:1103.5930 [hep-ph]
12. A. Dueck, S. Petcov, W. Rodejohann, Phys. Rev. D **82**, 013005 (2010). arXiv:1006.0227 [hep-ph]
13. Z.-z. Xing, S. Zhou, Phys. Lett. B **666**, 166 (2008). arXiv:0804.3512 [hep-ph]
14. P. Zucchelli, Phys. Lett. B **532**, 166 (2002)
15. C. Volpe, in *Proceedings of 13th Lomonosov Conference on Elementary Particles: Particle Physics on the Eve of the LHC*, Moscow, 2007, pp. 146–153. arXiv:0802.3352 [hep-ph]
16. C. Volpe, Prog. Part. Nucl. Phys. **64**, 325 (2010). arXiv:0911.4314 [hep-ph]
17. C. Orme, JHEP **1007**, 049 (2010). arXiv:0912.2676 [hep-ph]
18. P. Coloma, A. Donini, P. Migliozzi, L. Scotto Lavina, F. Terranova, Eur. Phys. J. C **71**, 1674 (2011). arXiv:1004.3773 [hep-ph]
19. J. Bernabeu, C. Espinoza, C. Orme, S. Palomares-Ruiz, S. Pascoli, AIP Conf. Proc. **1222**, 174 (2010)
20. S.K. Agarwalla, A. Raychaudhuri, A. Samanta, Phys. Lett. B **629**, 33 (2005). hep-ph/0505015
21. S.K. Agarwalla, S. Choubey, A. Raychaudhuri, Nucl. Phys. B **798**, 124 (2008). arXiv:0711.1459 [hep-ph]
22. S.K. Agarwalla, P. Huber, Phys. Lett. B **693**, 114 (2010). arXiv:0909.2257 [hep-ph]
23. D. Meloni, O. Mena, C. Orme, S. Palomares-Ruiz, S. Pascoli, JHEP **0807**, 115 (2008). arXiv:0802.0255 [hep-ph]
24. D. Meloni, O. Mena, C. Orme, S. Pascoli, S. Palomares-Ruiz, PoS NUFACT **08**, 133 (2008)
25. S.K. Agarwalla, Y. Kao, T. Takeuchi, arXiv:1302.6773 [hep-ph]
26. M. Blennow, A.Y. Smirnov, Adv. High Energy Phys. **2013**, 972485 (2013). arXiv:1306.2903 [hep-ph]
27. T.R. Edgecock, O. Caretta, T. Davenne, C. Densham, M. Fitton, D. Kelliher, P. Loveridge, S. Machida et al., Phys. Rev. ST Accel. Beams **16**, 021002 (2013). arXiv:1305.4067 [physics.acc-ph]
28. P. Huber, M. Lindner, M. Rolinec, W. Winter, Phys. Rev. D **73**, 053002 (2006). hep-ph/0506237
29. M. Mezzetto, J. Phys. G **29**, 1771 (2003). hep-ex/0302007
30. W. Winter, Phys. Rev. D **78**, 037101 (2008). arXiv:0804.4000 [hep-ph]
31. S.K. Agarwalla, S. Choubey, A. Raychaudhuri, W. Winter, JHEP **0806**, 090 (2008). arXiv:0802.3621 [hep-ex]
32. P. Huber, M. Lindner, W. Winter, Comput. Phys. Commun. **167**, 195 (2005). hep-ph/0407333
33. P. Huber, J. Kopp, M. Lindner, M. Rolinec, W. Winter, Comput. Phys. Commun. **177**, 432 (2007). hep-ph/0701187
34. M.C. Gonzalez-Garcia, M. Maltoni, J. Salvado, T. Schwetz, JHEP **1212**, 123 (2012). arXiv:1209.3023 [hep-ph] (see also, v1.1 results in http://www.nu-fit.org)
35. E.K. Akhmedov, S. Razzaque, AYu. Smirnov, JHEP **02**, 082 (2013). arXiv:1205.7071 [hep-ph]
36. S.K. Agarwalla, T. Li, O. Mena, S. Palomares-Ruiz, arXiv:1212.2238 [hep-ph]
37. D. Franco et al., JHEP **1304**, 008 (2013). arXiv:1301.4332 [hep-ex]
38. T. Ohlsson, H. Zhang, S. Zhou, Phys. Rev. D **88**, 013001 (2013). arXiv:1303.6130 [hep-ph]
39. A. Esmaili, AYu. Smirnov, JHEP **1306**, 026 (2013). arXiv:1304.1042 [hep-ph]
40. M. Ribordy, A.Y. Smirnov, Phys. Rev. D **87**, 113007 (2013). arXiv:1303.0758 [hep-ph]
41. W. Winter, Phys. Rev. D **88**, 013013 (2013). arXiv:1305.5539 [hep-ph]
42. M. Blennow, T. Schwetz, JHEP **1309**, 089 (2013). arXiv:1306.3988 [hep-ph]
43. S.K. Agarwalla, S. Prakash, S.U. Sankar, JHEP **1307**, 131 (2013). arXiv:1301.2574 [hep-ph]
44. F. Capozzi, E. Lisi, A. Marrone, arXiv:1309.1638 [hep-ph]
45. D.V. Forero, M. Tortola, J.W.F. Valle, Phys. Rev. D **86**, 073012 (2012). arXiv:1205.4018 [hep-ph]
46. S.K. Raut, Mod. Phys. Lett. A **28**, 1350093 (2013). arXiv:1209.5658 [hep-ph]
47. A.M. Dziewonski, D.L. Anderson, Preliminary reference earth model. Phys. Earth Planet Inter. **25**, 297 (1981)
48. F.F. Stancy, *Physics of the Earth*, 2nd edn. (Wiley, London, 1977)
49. A. Jansson, O. Mena, S.J. Parke, N. Saoulidou, Phys. Rev. D **78**, 053002 (2008). arXiv:0711.1075 [hep-ph]
50. P. Huber, M. Lindner, W. Winter, Nucl. Phys. B **645**, 3 (2002). hep-ph/0204352
51. L. Agostino et al. [MEMPHYS Collaboration], JCAP **1301**, 024 (2013). arXiv:1206.6665 [hep-ex]
52. M.D. Messier, UMI-99-23965
53. E.A. Paschos, J.Y. Yu, Phys. Rev. D **65**, 033002 (2002). hep-ph/0107261
54. A.A. Aguilar-Arevalo et al. [MiniBooNE Collaboration], Phys. Rev. D **88**, 032001 (2013). arXiv:1301.7067 [hep-ex]
55. P. Huber, M. Lindner, W. Winter, Comput. Phys. Commun. **167**, 195 (2005). hep-ph/0407333
56. P. Huber, J. Kopp, M. Lindner, M. Rolinec, W. Winter, Comput. Phys. Commun. **177**, 432 (2007). hep-ph/0701187
57. S. Childress, J. Strait, J. Phys. Conf. Ser. **408**, 012007 (2013)
58. A. Stahl, C. Wiebusch, A.M. Guler, M. Kamiscioglu, R. Sever, A.U. Yilmazer, C. Gunes , D. Yilmaz et al., CERN-SPSC-2012-021